15th Canadian Masonry Symposium
Ottawa, Canada
June 2-5, 2025

Structural Vulnerability Assessment of a CMU-PG Reinforced Masonry Building

Sebastián Calderón[i], Benjamín Ruz[ii], Rosita Jünemann[iii], Cristián Jaque[iv], Cristián Sandoval[v], Pablo Heresi[vi], Gonzalo Montalva[vii], Felipe Leyton[viii]

ABSTRACT

In Chile, a great part of residential buildings are made of masonry, many of them reinforced or confined, partially grouted, and typically up to four stories high. In general, these buildings are structured in walls, making them very stiff and prone to fail in shear when subjected to lateral loads. This type of failure is of particular interest in the country due to its high seismic activity, implying that evaluating the seismic vulnerability of this type of building has always been a concern. Despite this, performing vulnerability evaluations of this type of building is uncommon in the country.

Different approaches have been proposed to perform vulnerability analyses and evaluate the response of a building under different earthquake scenarios and its most damage-susceptible structural elements. Recent studies have implemented numerical models to assess the seismic vulnerability of multi-story buildings, although these studies only focus on the performance of fully grouted masonry structures. The grouting type in masonry significantly impacts the material's behavior and performance, meaning that appropriate models must be developed for assessing partially grouted masonry.

In response to this gap, a case study four-story concrete masonry unit reinforced masonry building is numerically modeled to evaluate its structural vulnerability. The model is implemented in OpenSees. The shear wall elements were simulated employing a non-linear macro model, which was validated against experimental results of walls available in the literature. Once the suitability of the modeling approach for each structural element was validated, their assembly representing the whole case study structure was employed to run nonlinear incremental dynamic analysis. The obtained results at the shear wall element level show the suitability of the approach, and the results at the whole structure model are coherent with failures reported in post-earthquake field inspections.

KEYWORDS

Nonlinear modeling, incremental dynamic analysis, concrete masonry unit, structural vulnerability

---

[i] Assistant Professor, Universidad de Concepción, Chile, sebastian.calderon@udec.cl
[ii] Masters' student, Universidad de Concepción, Chile, bruz2018@udec.cl
[iii] Assistant Professor, Pontificia Universidad Católica de Chile, Chile, rjunemann@uc.cl
[iv] Masters' student, Pontificia Universidad Católica de Chile, Chile, cjaquep@uc.cl
[v] Associate Professor, Pontificia Universidad Católica de Chile, Chile, Cristian.sandoval@uc.cl
[vi] Assistant Professor, Universidad de Chile, Chile, pheresi@uchile.cl
[vii] Associate Professor, Universidad de Concepción, Concepción, gmontalva@udec.cl
[viii] Researcher, Centro Sismológico Nacional, Universidad de Chile, Chile, leyton@csn.uchile.cl

INTRODUCTION

In Chile and Latin America, a large portion of residential buildings are made of masonry. One of the characteristic archetypes of Chilean masonry buildings corresponds to flat buildings up to four stories in height composed of four to six units of about 32 to 55 m^2 per floor. Usually, they are structured in shear walls tied together by reinforced concrete slabs (typically 12 cm thick), which results in very stiff structures. The walls can be either confined or reinforced masonry (RM). In the case of RM, the common practice in the country is only grouting vertical cells containing vertical reinforcement (i.e., partial grouting, PG) and using horizontal reinforcement embedded in bed joints (bed-joint reinforcement, BJR). The use of BJR-PG-RM as structural elements and the layout of the building makes them prone to failure in shear when subjected to lateral loads [1]. This type of failure is of particular interest in the country due to its high seismic activity, implying that evaluating the seismic vulnerability of this type of building has always been a concern. Despite this, performing vulnerability evaluations of this type of building is uncommon in the country.

Different approaches have been proposed to perform vulnerability analyses and evaluate the response of masonry buildings under different earthquake scenarios and its most damage-susceptible structural elements. Recent studies have implemented numerical models to assess the seismic vulnerability of multi-story buildings. Siyam et al. [2] and Ezzeldin et al. [3] adequately perform vulnerability assessments following the performance-based design methodology. In these studies, three-dimensional numerical models of floor systems were developed, which were able to capture the non-linearity of the structural elements. However, these studies focus on fully grouted wall typologies, which behave differently from PG walls. On the other hand, Ramírez [4] proposed a simplified approach to evaluate the response of BJR-PG-RM buildings, adopting three degrees of freedom per story, assuming that there is a rigid diaphragm. In that study, the behavior of each wall was simulated with the Smooth-Hysteretic model [5], adopting parameters from either experimental results or numerical simulations. The obtained results permitted assessing the damage level that the structure underwent, although the major issue was associated with the accuracy of the model adopted for each wall.

As exposed, the approaches to simulate the seismic behavior of BJR-PG-RM for risk assessments are limited. In response to this, this study proposes a simplified approach to evaluate the seismic vulnerability of this type of structure. A four-story concrete block reinforced masonry building structured in shear walls of concrete masonry units (CMUs) is adopted as a case study. The walls are simulated with a nonlinear uniaxial constitutive law, whose parameters are varied according to the properties of the elements. Then a single-record incremental dynamic analysis (IDA) is carried out employing the nonlinear models and a selected ground motion to evaluate the suitability of the model. The results of a nonlinear time-history analysis using a particular scale factor are analyzed to verify the behavior of different elements in detail.

METHODOLOGY

The purpose is to generate a model of BJR-PG-RM structures capable of representing their nonlinear cyclic behavior as simply as possible. Given the recognized complex behavior of this typology, some reasonable simplifications were adopted to avoid requiring extremely detailed models, which implies some accuracy concessions that do not compromise the representativity of the assessed buildings. The models were implemented using OpenSeesPy [6] as a combination of one DOF (degree of freedom) springs oriented in the two principal directions of the building (longitudinal and transversal, X and Y, respectively). Each wall element was represented by a two-node link element that connected the bottom and top geometrical centers of the walls. These link elements only work in the in-plane and out-of-plane direction of the structural element, as schematically shown in Fig 1. Given that the floor systems of the represented types of structures are usually concrete slabs, a rigid diaphragm condition was assumed for each floor, which was implemented by employing geometrical restrictions.

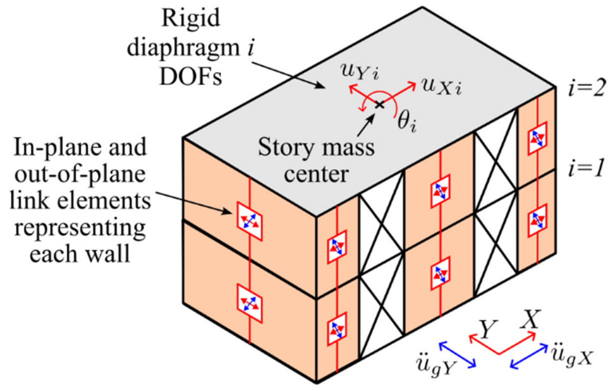

Figure 1. Modeling approach.

Given the target type of building to be modeled and the failure modes observed after earthquakes, it has been identified that the in-plane shear response controls the structural performance. Therefore, as the focus is a simple structural model, the nonlinear in-plane shear behavior of the walls was simulated employing the hysteretic model proposed by Mazzoni [7]. This model represents a uniaxial multilinear hysteretic material object that incorporates force and deformation pinching, accounts for damage caused by ductility and energy, and exhibits reduced unloading stiffness as a function of ductility. The curve is defined by an envelope of up to seven points in the push and pull loading directions and five parameters that modify the hysteresis shape. The envelope and hysteresis parameters should be modified according to the properties of each wall, as described below.

The mass of the model was estimated from the self-weight of the different elements in the building (structural and nonstructural). The mass was considered concentrated at the geometrical center of each floor, considering the layout of the building. Extra viscous damping was incorporated to account for the influence of non-structural components and other neglected structural contributions (e.g., out-of-plane bending) and to stabilize the numerical response of the models. A Rayleigh damping based on the mass matrix was used for this purpose, with a coefficient calibrated to represent 5% of the critical damping ratio for the fundamental elastic translational vibration mode of the building.

There are two possible approaches to evaluate the hysteresis model of each wall: the calibration of parameters of the constitutive law to meet a specific shape, or using scaling factors of already calibrated curves. Both approaches are explained below.

Calibration of parameters to represent wall elements

The first option is adjusting the constitutive law parameters to meet a known shape, which might come from experimental results of cyclic tests of walls with similar properties or from results of more detailed numerical models. In this study, the hysteretic model of the walls was calibrated against experimental results reported by Calderón et al. [8] because the tested specimens have a similar layout, material strength, and axial load to some of the walls of the study case.

As an example of the adjustment procedure, the squared wall of Fig. 2 is presented. First, the points of the envelope hysteretic model were chosen to approximate the experimentally measured envelope. Then, the displacement pattern used in experimental tests was applied to the model, monitoring the reaction force. Then, the five hysteresis parameters required by the model were modified to minimize the quadratic difference between the cumulative energy of the test and the numerical simulation. It is worth mentioning that this optimization procedure was automated by using the BFGS method [9].

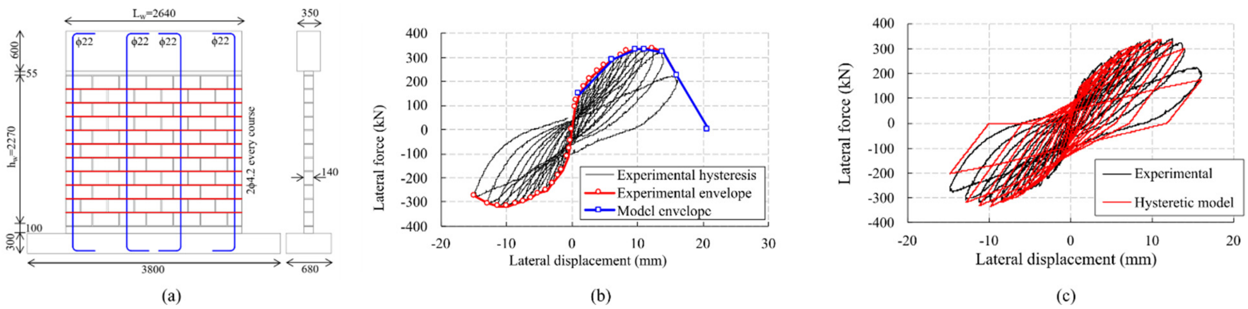

Figure 2. Example of calibration procedure of hysteretic model: (a) reference wall [8], (b) selection of envelope points, (c) hysteresis curve.

Scaling factors for simplified representation

The second alternative is to adopt rules to scale the shape of already calibrated hysteresis curves of a reference wall. For instance, forces and displacements of the envelope of a similar wall can be modified by factors dependent on the differences between the two walls. One alternative for the modification factor of forces is the ratio between the estimated maximum force of the simulated wall and the maximum force exhibited by the reference wall. There are different expressions in the literature that can be used to estimate the strength of walls, such as that proposed by Calderón et al. (2022), which is suitable for BJR-PG-RM shear walls (Eq. (1)). In the equation, A_n, A_{sht}, A_{svt} are the net cross-sectional area of the wall, the total horizontal reinforcement area, and the total vertical reinforcement area, respectively (all in mm^2); d_v is the effective depth of the wall in mm (distance from the most extreme compression fiber to the centroid of the farthest vertical reinforcement); $f'_{m,n}, f_{yh}$, f_{yv} are the compressive strength of masonry calculated on the net area, the yield stress of the horizontal and vertical reinforcement, respectively (all in MPa); P and V are the axial load and in-plane shear force applied in N; M is the bending moment within the applied plane in $N \cdot mm$. The first term of Eq. (1) is associated with the masonry contribution, the second to the axial load, the third to the horizontal reinforcement, and the last to the vertical reinforcement. It should be met that the axial load contribution cannot be greater than that of the masonry and that the steel reinforcement contribution cannot be greater than that of the first two terms.

$$(1)\quad V_n = 0.1023 \cdot A_n\sqrt{f_{m,n}} + \left(0.123 + 0.3063\left(\frac{M}{V \cdot d_v}\right)^{-1}\right)P + 0.5 \cdot \frac{A_{sht}}{h_w} f_{yh} \min\,(h_w, L_w) + 0.0485 \cdot A_{svt} f_{yv}$$

$$(2)\quad \alpha_\delta = \overline{\delta_{Vmax,obj}} \big/ \overline{\delta_{Vmax,ref}}$$

Calderón et al. [1] [8] gathered a database of experimental tests of CMU BJR-PG-RM walls, and grouped the database in three ranges of aspect ratios (squat, squared, and slender), as indicated in Table 1. The authors indicated that shear displacement capacity tends to be proportional to the wall aspect ratio, although variability is significant, and greater differences are between squat and squared walls than between squared and slender walls. Accordingly, deformations were scaled in this study using the factor α_δ, defined in Eq. (2). In the expression, $\overline{\delta_{Vmax,obj}}$ stands for the average displacement at the shear capacity of walls in the group of the modeled wall. While, $\overline{\delta_{Vmax,ref}}$ is for the average displacement at the shear capacity of walls in the group of the reference wall. The calculated factors are presented in Table 1.

Table 1: Factors to scale load-displacement deformations.

Reference wall		Displacement / story-drift ratio scaling factor for simulated wall		
Wall type	Aspect ratio (h_w/L_w)	Squat wall ($h_w/L_w < 0.8$)	Squared wall ($0.8 \leq h_w/L_w \leq 1.1$)	Slender wall ($h_w/L_w > 1.1$)
Squat	<0.8	1.00	2.01	2.59
Squared	[0.8;1.1]	0.50	1.00	1.29
Slender	>1.1	0.39	0.78	1.00

DESCRIPTION OF CASE STUDY

A four-story housing complex of BJR-PG-RM of Concrete Masonry Units (CMUs) was selected. A similar building was adopted as case study by Calderón et al. [10]. The case study has a typical story plan of 17.7 m long and 6.4 m wide (Fig. 3(a)), with a reinforced concrete slab of 12 cm and a typical story height of 2.47 m. The floor plan configuration is regular and symmetrical in the Y direction through reference axis 3, while there is little asymmetry in the X direction. The typical story is formed by 24 walls, which are coded as WX (X: wall number), as presented in Fig. 3(a). Some of them have the same configuration, given the symmetry of the building. Thus, walls are grouped into 11 types, whose geometrical characteristics are presented in Table 2. It also can be mentioned that doors and windows tend to be concentrated in the X direction of the structure, resulting in wall configurations of shorter length and higher aspect ratio than in the Y direction, as exemplified in Fig. 3(b). The fundamental periods of the buildings are 0.169 s in the X-direction, and 0.143 s in the Y-direction.

Table 2: Properties of walls.

Wall type	Direction	Wall codes	Length (cm)	Aspect ratio	Displacement correction factor	Expected displacement at shear capacity (mm)	Estimated shear capacity (kN)	Force correction factor
1	X	W1, W8, W11, W17	108	2.18	1.29	15.75	105.09	0.31
2	X	W2, W7	148	1.59	1.29	15.75	144.56	0.43
3	X	W3, W6	98	2.40	1.29	15.75	95.27	0.28
4	X	W4, W5	50	4.70	1.29	15.75	48.38	0.14
5	X	W9, W10	214	1.10	1	12.21	210.33	0.62
6	X	W12, W16	215	1.09	1	12.21	211.33	0.62
7	X	W13, W15	99	2.37	1.29	15.75	96.25	0.28
8	X	W14	280	0.84	1	12.21	276.90	0.82
9	Y	W18, W21, W24	642	0.37	0.5	6.11	492.53	1.46
10	Y	W19, W22	164	1.43	1.29	15.75	160.43	0.47
11	Y	W20, W23	280	0.84	1	12.21	276.90	0.82

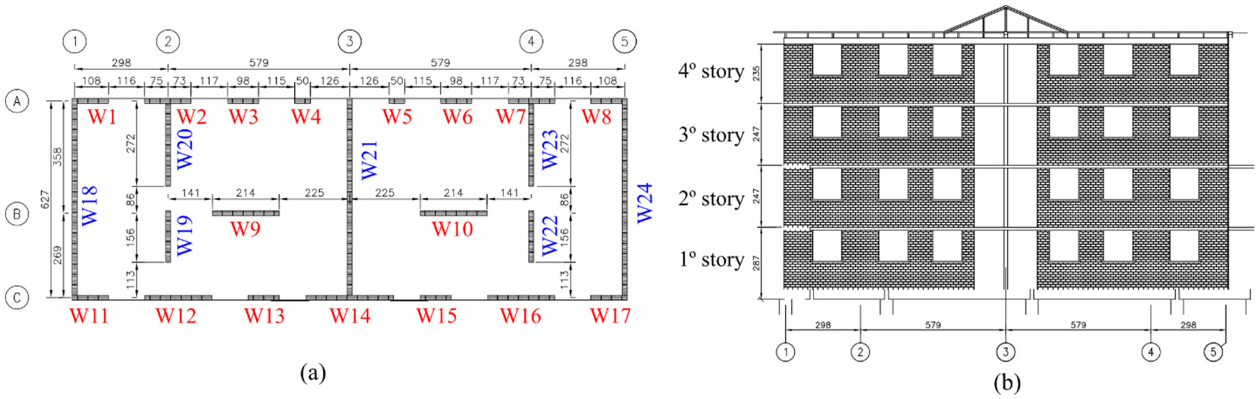

Figure 3. Case study: (a) typical story plan view, (b) frontal view.

The CMUs are 14 cm thick, 29 cm long, and 19 cm high. The typical horizontal reinforcement corresponded to ladder-type reinforcement at every joint, each made of 2 longitudinal 4.2 mm diameter rebars, crossties at every 30 cm. As per vertical reinforcement, rebars of 12 mm were specified for wall edges, and in between 10 mm diameter rebars separated at 50 cm (generally) were indicated between edges. The above resulted in typical horizontal and vertical reinforcement ratios of 0.049% and 0.11%, respectively. Regarding material properties, the specified masonry compressive strength is 2.5 MPa (based on gross cross-section), a steel grade AT560-500 was indicated for horizontal reinforcement. These properties were employed to use the calibration approach to represent a squared wall, and then the adjusted constitutive law was modified to represent each wall of the building using the scaling factors approach.

A single-record IDA was carried out using the ground motion recorded at the location of the building (Constitución, Chile) during the M_w8.8 Maule 2010 earthquake, whose components are shown in Fig. 4. In this case, the North-South component was aligned with the Y-direction of the building and the East-West with the X-direction. Both record components were applied simultaneously.

Two EDPs (Engineering Damage Parameters) were assessed for each wall: SDR (Story-Drift Ratio) and NDSD (Normalized Diagonal Shear Demand), as in [1]. The SDR is calculated as the inter-story displacement divided by the height of the wall. The NDSD is calculated as the in-plane shear demand divided by the nominal shear capacity.

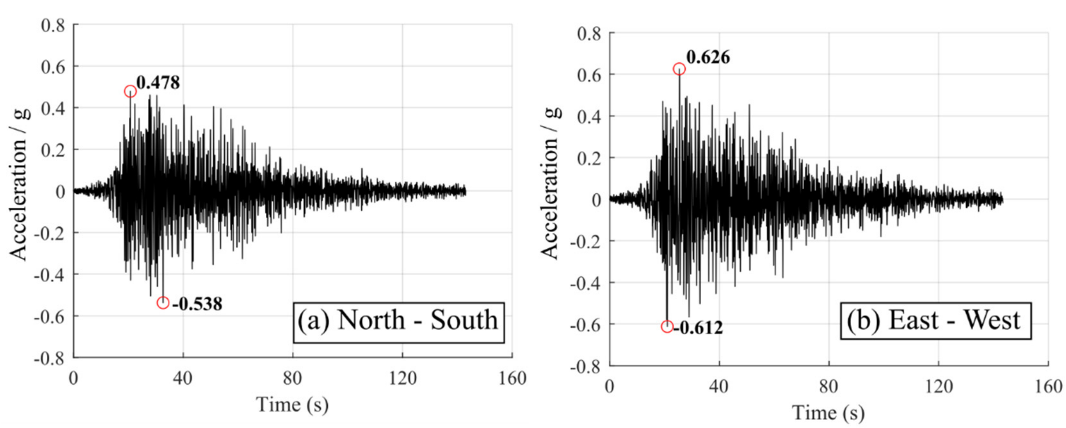

Figure 4. Seismic record components.

RESULTS

Single-record incremental dynamic analysis

The IDA considered PGA values up to 0.39g, which was achieved by scaling the records by factors up to 0.626. It is worth mentioning that the model did not converge for higher scaling factors due to excessive displacement and shear forces. The latter can be physically interpreted as an extreme damage status, which can be linked to the collapse of the structure or irrecuperable damage leading to the demolition of the building.

Results of this analysis for the first floor are presented in Fig. 5(a-b) and first-story walls in Fig. 5(c-d). The mass center SDR (Story-Drift Ratio) grows steadily linear up to a PGA/g of 0.25, when the increment rate of the SDR of the first story in the X-direction exhibits a drastic variation. A similar behavior is observed in the Y-direction at a PGA/g of 0.38. This difference might be attributed to the higher PGA that the components of the seismic records impose in the X-direction than in the Y-direction, which is 16.4% higher. Regarding the basal shear normalized by the shear capacity in the analysis direction, a linear increment is observed in both components, approximately up to a PGA/g equal to 0.28. Then, the rate of increment decreases in the X-direction, indicating that some wall elements reach their shear capacity. This behavior is later observed in the Y-direction at PGA/g of 0.38, which can also be connected to the smaller demands imposed in the Y-direction compared to the X-direction for the same scale factor. A similar trend can be observed in Fig. 5(c-d) when comparing the EDPs (both SDR and NDSD) developed by selected walls in the X-direction (walls 1, 9, 11, and 14) with those in the Y-direction (walls 18, 20, 21, and 24). The evolution of SDR in wall elements (Fig. 5(c)) is directly related to the diaphragm mass center SDR (Fig. 5(a)). Only some differences can be noticed for walls in the Y-direction at elevated PGA/g values. This latter indicates that the rotation of the diaphragm increases and becomes significant when the seismic demand is high enough to produce severe damage in different wall elements. The evolution of the NDSD of each wall indicates that the most critical elements are walls 1 and 11, both aligned with the X-direction. These walls exhibit an increased variation in the NDSD for PGA/g values higher than 0.28, corroborating that the X-direction controls the obtained response. Nonetheless, when the PGA is about 0.35g, wall 20 (oriented in the Y-direction) shows a steeped increment. This increment indicates that demands in the X-direction walls are enough to require other elements in the perpendicular direction of analysis.

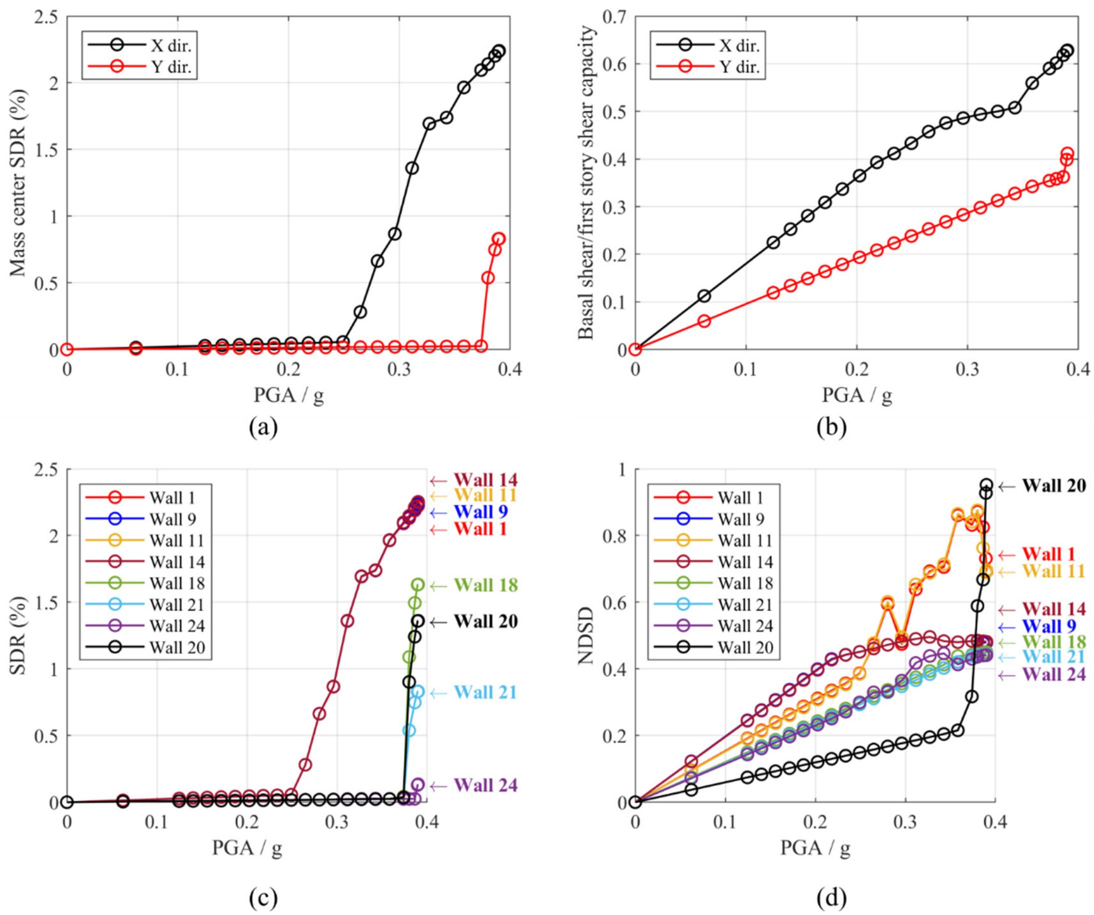

Figure 5. Single-record IDA results: (a) inter-story drift ratio of the mass center, (b) basal shear demand-to-first story shear capacity ratio, (c) SDR for selected walls, (d) NDSD for selected walls.

Nonlinear time-history analysis results

The seismic records scaled to reach a PGA/g of 0.272 (scale factor of 0.4347) are used to analyze the time-history response of the structure and certain walls in detail. This PGA produces a maximum SDR approximately equal to 0.45% in walls 1, 9, 11, and 14 (X-direction aligned walls), which corresponds to the mean of the DS5 SDR-based fragility functions for CMU proposed for Chilean BJR-PG-RM proposed by Calderón et al. [1]. Table 3 summarizes the maximum values of some structural outputs. The basal shear is plotted in Fig. 6(a), while SDR corresponding to the different story diaphragm mass centers are presented in Fig. 6(b-d) (D*i*, where *i* corresponds to the story number). As expected, the structure exhibits higher shear demands in the X-direction than in the Y-direction (Fig. 6(a)). In the X-direction, the instant at which the highest shear forces are observed does not match the instant at which the highest SDR on the first floor (diaphragm D1) are observed (Fig. 6(b)), indicating cumulated damage because of walls hysteresis. It also can be observed that interstory deformations mostly concentrate on the first floor. On the other hand, the basal shear in the Y-direction correlates well with SDR experienced by diaphragm mass centers (Fig. 6(c)). Thus, in general, the damage in X-direction is not comparable to that of the Y-direction in this case. Fig. 6(d) depicts the relationship between the SDR attained in both analysis directions at different instants. In general, the maximum deformations do not tend to be coupled in both directions, at least on the first floor, since the time frames of maximum values are not in phase between analysis directions. Some coupling can be observed on diaphragms 2 to 4, but SDRs are generally small in these elements.

Table 3: Structure outputs for a PGA/g of 0.272.

Diaphragm	Direction	Mass center displacement (mm)	Story deformation (mm)	Drift ratio (%)
1	X	8.11	8.11	0.34
	Y	0.42	0.42	0.02
2	X	8.32	1.06	0.05
	Y	0.74	0.32	0.01
3	X	8.45	0.7	0.03
	Y	0.95	0.21	0.01
4	X	8.49	0.24	0.01
	Y	1.02	0.07	0.003

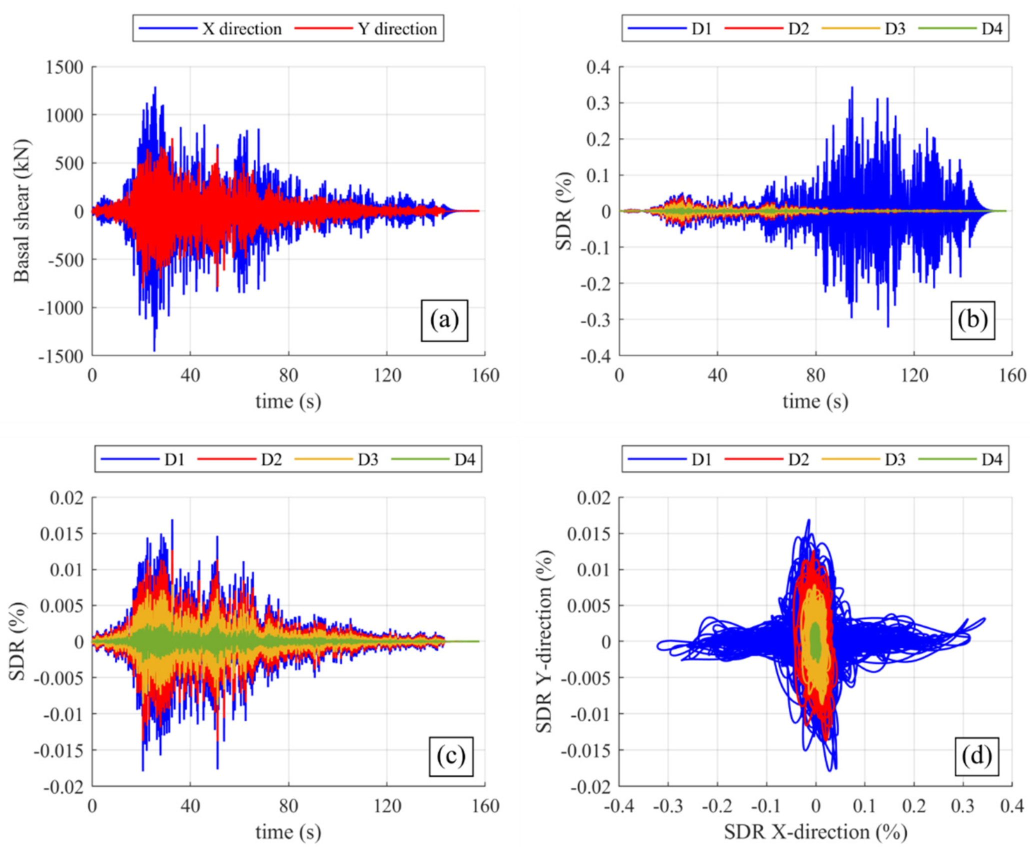

Figure 6. Structure response for a PGA/g of 0.272: (a) Basal reactions, (b) X direction interstory displacements, (c) Y direction interstory displacements, (d) interstory displacements.

The hysteretic in-plane response of interest walls is depicted in Fig. 7, and notable output variables are summarized in Table 4. In general, it can be observed that walls aligned with the X-direction behave nonlinearly (Fig. 7(a-d)), while the selected walls in the Y-direction remain linear (Fig. 7(e-h)). It also can be noted that walls 1, 9, 11, and 14 exhibit severe degradation, losing all their bearing capacity by the end of the NLTH analysis.

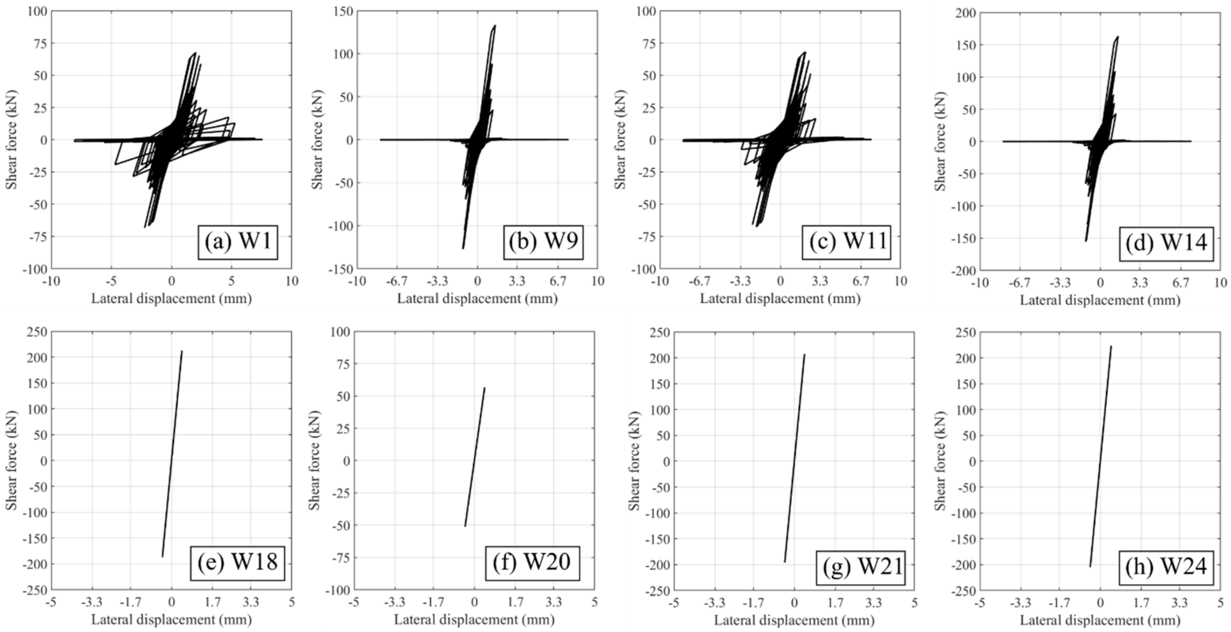

Figure 7. In-plane shear response of first story walls for a PGA/g of 0.272.

The above results imply that many elements reach a severe damage state. In this situation, the building poses safety issues to occupants, requiring immediate repair measures, such as the total replacement of structural elements or demolishing the entire building if the damage is too extensive.

Table 4: Response outputs of first story walls for a PGA/g of 0.272.

Wall	In-plane direction	Maximum deformation (mm)	Displacement capacity ratio (%)	Maximum shear force (kN)	Shear demand to capacity ratio, NDSD (%)
1	X	8.1	51.41	68.38	47.63
9	X	8.11	66.39	133.36	46.52
11	X	8.11	51.51	68.18	47.5
14	X	8.11	66.44	163.25	46.52
18	Y	0.43	7.07	212.44	32.58
20	Y	0.42	6.91	207.54	31.82
21	Y	0.45	7.44	223.45	34.26
24	Y	0.43	3.51	56.71	16.16

CONCLUSIONS

This study presented a simplified methodology for simulating the seismic behavior of partially grouted reinforced masonry structures, with a case study of a four-story concrete masonry unit building. A nonlinear single-record incremental dynamic analysis was carried out. The model for each wall element was calibrated using experimental data from cyclically tested walls. Results at the individual wall element level demonstrate the effectiveness of this approach. Furthermore, the overall structural model results align with damage patterns observed in post-earthquake field inspections.

In addition to the efficiency of the simplified model, its ability to perform multiple analyses quickly is noteworthy, enabling the assessment of various acceleration records. This feature could be valuable for inclusion in future studies to explore different seismic hazard scenarios. Given the promising results and the generalizability of the methodology, future studies may explore its applicability to other masonry types, such as fully grouted reinforced masonry and confined masonry.

ACKNOWLEDGEMENTS

The authors acknowledge the support of EASER (Evolution Assessment of Seismic Risk) project under grant number ACT240044 from the National Agency for Research and Development (ANID). The authors also acknowledge the support of projects FONDECYT Iniciación No. 11230388 and FONDECYT Iniciación No. 11230463 from the National Agency for Research and Development (ANID).

REFERENCES

[1] Calderón S, Vargas L, Sandoval C, Araya-Letelier G, Milani G. (2022). Shear design equation and updated fragility functions for partially grouted reinforced masonry shear walls. *Journal of Building Engineering*, 50, 104097. https://doi.org/10.1016/j.jobe.2022.104097.

[2] Siyam MA, Konstantinidis D, El-Dakhakhni W. (2016). Collapse Fragility Evaluation of Ductile Reinforced Concrete Block Wall Systems for Seismic Risk Assessment. *Journal of Performance of Constructed Facilities*, 30. https://doi.org/10.1061/(ASCE)CF.1943-5509.0000895.

[3] Ezzeldin M, Wiebe L, El-Dakhakhni W. (2017). System-Level Seismic Risk Assessment Methodology: Application to Reinforced Masonry Buildings with Boundary Elements. *Journal of Structural Engineering*, 143. https://doi.org/10.1061/(ASCE)ST.1943-541X.0001815.

[4] Ramírez P. (2021). *Análisis de fragilidad sísmica de edificaciones de albañilería armada.* PhD Thesis. Pontificia Universidad Católica de Chile.

[5] Sivaselvan M, Reinhorn A. (2000). Hysteretic Models for Deteriorating Inelastic Structures. *J Eng Mech*, 126, 633–640.

[6] Pacific Earthquake Engineering Research Center (PEER). (2024). OpenSeesPy.

[7] Mazzoni S. (2022) HystereticSM Material. https://OpenseesGithubIo/OpenSeesDocumentation/User/Manual/Material/UniaxialMaterials/HystereticSMHtml.

[8] Calderón S, Vargas L, Sandoval C, Araya-Letelier G. (2020). Behavior of Partially Grouted Concrete Masonry Walls under Quasi-Static Cyclic Lateral Loading. *Materials*, 2020, 13, 2424. https://doi.org/10.3390/ma13102424.

[9] SciPy. (2024). SciPy library.

[10] Calderón S, Sandoval C, Aguilar V, Vargas L, Araya-Letelier G. Diseño a corte basado en resistencia para muros de albañilería armada. (2023). Una propuesta de actualización de la norma NCh 1928. *XIII Congreso Chileno de Sismología e Ingeniería Sísmica (ACHISINA)*, Viña Del Mar, Chile.